
SPHINX: Structural Prediction using Hypergraph Inference Network

Iulia Duta
University of Cambridge
id366@cam.ac.uk

Pietro Liò
University of Cambridge
pl219@cam.ac.uk

Abstract

The importance of higher-order relations is widely recognized in a large number of real-world systems. However, annotating them is a tedious and sometimes impossible task. Consequently, current approaches for data modelling either ignore the higher-order interactions altogether or simplify them into pairwise connections. In order to facilitate higher-order processing, even when a hypergraph structure is not available, we introduce Structural Prediction using Hypergraph Inference Network (SPHINX), a model that learns to infer a latent hypergraph structure in an unsupervised way, solely from the final node-level signal. The model consists of a soft, differentiable clustering method used to sequentially predict, for each hyperedge, the probability distribution over the nodes and a sampling algorithm that converts them into an explicit hypergraph structure. We show that the recent advancement in k -subset sampling represents a suitable tool for producing discrete hypergraph structures, addressing some of the training instabilities exhibited by prior works. The resulting model can generate the higher-order structure necessary for any modern hypergraph neural network, facilitating the capture of higher-order interaction in domains where annotating them is difficult. Through extensive ablation studies and experiments conducted on two challenging datasets for trajectory prediction, we demonstrate that our model is capable of inferring suitable latent hypergraphs, that are interpretable and enhance the final performance.

1 Introduction

Graph data is universally recognized as the standard representation for relational data. However, their capabilities are restricted to only modelling pairwise connections. Emerging research shows that real-world applications including neuroscience [1, 2], chemistry [3], biology [4], often exhibit group interactions, involving more than two elements. This leads to the development of a new field dedicated to representing higher-order relations, in the form of hypergraphs.

However, while graph datasets are widespread in the machine learning community [5, 6], the availability of hypergraph datasets is much more limited. Recent work [7] highlights two potential causes for the lack of higher-order data. On one hand, current technology used for collecting information are mostly designed or optimised to detect pairwise interactions. Furthermore, even in the exceptional cases when the data is gathered in a higher-order format, the published version is often released in a reduced, pairwise form.

Therefore, to preserve the higher-order information, it is crucial to develop methods for learning the hypergraph structure in an unsupervised way, only from point-wise observations. Motivated by this, we introduce Structural Prediction using Hypergraph Inference Network (SPHINX), a model for unsupervised latent hypergraph inference, that can be used in conjunction with any recent models designed for hypergraph processing. SPHINX models the hyperedge discovery as a clustering problem, adapting a soft clustering algorithm to sequentially identify subsets of highly-correlated

nodes, corresponding to each hyperedge. To produce a discrete hypergraphs structure, we take advantage of the recent development in differentiable k -subset sampling [8, 9], obtaining a more effective training procedure, that eliminates the necessity for heavy regularisation. While classical selection methods such as Gumbel-Softmax [10] fail to control the sparsity of the hypergraph, our constrained k -subset sampling produces more accurate latent structure.

Our model improves the relational processing by learning an appropriate hypergraph structure for the downstream task, without any supervision at the structure level. Our experiments on trajectory prediction show that the inferred structure correlates well with the ground-truth connectivity that guides the dynamical process, while also being beneficial for improving the performance on the higher-level task. The resulting model is general, easy to optimise, which makes it an excellent candidate for modelling higher-order relations, even in the absence of an annotated connectivity.

Our main contributions are summarised as follow:

1. We propose a **novel method for explicit hypergraph inference**, that uses a sequential, differentiable clustering approach for identifying subsets of highly-related nodes and a k -subset sampling to produce an explicit hypergraph structure, that can be plugged into any hypergraph neural network.
2. The model performs **unsupervised hypergraph discovery**, by using supervision only from the weak node-level signal. We empirically show that the predicted hypergraph correlates well with the true higher-order structure, even if the model was not optimised for this task.
3. The latent hypergraph inference enforces an **inductive bias towards capturing higher-order correlations**, even in the absence of the real structure, which proved to be **beneficial for high-level tasks** such as trajectory prediction. Having an explicit structure enables us to visualise the discovered hypergraph, adding another layer of interpretability into the model.

2 Related work

Structural inference on graph. Modelling relational data using Graph Neural Networks (GNNs) [11, 12] proves to be beneficial in several real-world domains including healthcare [13], physics [14], weather forecast [15], mathematics [16], sports analysis [17], chemistry [18] and many more. Most of the current graph methods assume that the graph connectivity is known. However, providing the relational structure is a highly challenging task, that, when possible to compute, requires either expensive tools, or advanced domain knowledge. These limitations led to the development of a new machine learning field dedicated to learning to infer structure from data in an unsupervised way.

Neural Relational Inference [19] is one of the pioneering works inferring an adjacency matrix from point-wise observations. The model consists of an encoder that learns to predict a distribution over the potential relationships and a GNN decoder that receives a sampled graph structure and learn to predict the future trajectory. fNRI [20] extends this work by inferring a factorised latent space, capable to encode multiple relational types, while [21] incorporates causal relations into the framework. When using temporal data, these models infer a single structure for the entire timeseries. dNRI [22] improves on that respect, by modifying the graph structure at each timestep.

Hypergraph Networks. While being a versatile, widespread data structure, graphs are constrained to only represent pairwise connections. Many real-world events contains higher-order interactions, where a relationship contains more than two elements. Several data structures for higher-order modelling were proposed in mathematics, including simplicial complexes [23], cell complexes [24], and more generally, hypergraphs [25]. To model hypergraphs, several deep learning methods have recently emerged. Hypergraph Neural Networks [26] applies GNNs on top of a weighted clique expansion. This could be seen as a two-stage message passing scheme. In the first stage the information is send from nodes to hyperedges, while in the second stage the messages are send back from hyperedges to nodes. UniGNN [27] and AllDeepSets [28] introduce a more general framework in which the two stages can be implemented as any permutation-invariant function such as GNNs, DeepSets [29] or Transformers [30]. Further proposed extensions include the integration of attention mechanisms [31–33], or attaching additional geometric structure to the hypergraph, through the incorporation of cellular sheaves [34].

Structural inference on hypergraphs. Providing the hypergraph structure to the model requires measuring higher-order correlations, which often implies a highly difficult and expensive annotation process. This leads to the necessity of inferring the hypergraph structure directly from data. However, when moving from the graph realm to the hypergraph domain, the set of potential edge candidates abruptly increases from quadratic to exponential. This makes the problem of inferring the latent hypergraph structure significantly more challenging. Classical attempts of achieving this includes methods based on Bayesian inference [35] or statistical approaches that compares against a null model for hypergraphs to filter the possible hyperedges [36].

While relational inference for graph data is an established field in deep learning, it remains largely unexplored in the hypergraph domain. Cellular complexes represent an alternative, hierarchical data structure for modelling higher-order relationships. DCM [37] performs structural inference for cellular complexes by proposing a method that learns to efficiently filter from the pool of all possible polygons associated with a graph. [38] proposes a supervised, iterative refinement method for set-to-hypergraph task, suitable for large input set sizes. For environments when a ground-truth hypergraph structure is not available, most of the existing methods focuses on the transductive setup, where a single hypergraph is inferred for the entire dataset. [39] treats the incidence matrix as a learnable parameter, while [40, 41] build a closed-form solution for the label propagation task.

On the other hand, for the inductive setup, where each example requires inferring a distinct hypergraph, the literature is very scarce. GroupNet [42] extracts a subset of nodes by identifying highly connected blocks in the correlation matrix. Alternatively, EvolveHypergraph [43] uses a GNN model to infer the probabilities of each node being part of a hypergraph and transform this into a hypergraph structure using a Gumbel-Softmax [10] sampling technique. While obtaining good results on the trajectory prediction tasks, properly optimising these methods requires a high degree of regularisation techniques, including auxiliary loss terms for reconstruction, smoothness or diversity. We believe that this mainly stems from challenges in effectively propagating gradients during the discretization phase. Gumbel-Softmax struggles to control the cardinality of the hyperedges, while top- k operations only partially tracks gradients. Moreover, these methods suffer a severe drop in performance when using only the hypergraph structure, with best performance requiring additional pairwise computation.

On the other hand, we are proposing a dedicated hypergraph-only model, that can be easily optimised solely from the final, downstream supervision, eliminating the need for additional optimisation heuristics. As we demonstrate in the experimental section, this advantage is brought by two important design choices: 1) the sequential differentiable-clustering which creates globally-informed probability distribution, alleviating the ambiguity existent in the hyperedge prediction problem and 2) adopting the k -subset sampling for discretizing the structure, a method that produces high-quality gradients for the constrained sampling operation. The resulting model is a versatile and general module, useful for hypergraph processing in scenarios where the hypergraph is not available.

3 Structure Prediction using Hypergraph Inference Network

The Structure Prediction using Hypergraph Inference Network (SPHINX) model is designed to produce higher-order representations without access to a ground-truth hypergraph structure. From the set of point-level observations, the model learns to infer a latent hypergraph that can be further used in conjunction with any classical hypergraph neural network architecture.

Our input consists of a set of nodes $V = \{v_i | i \in \{1 \dots N\}\}$, each one characterised by a feature vector $x_i \in \mathbb{R}^f$, which can either represent general characteristics of the nodes or, in our experiments, the summary of an observed T -seconds trajectory. The goal is to predict, for each node, the target $y_i \in \mathbb{R}^c$. In the entire paper, we are following the assumption that the node-level target y_i is the result of a higher-order dynamics, guided by an unknown higher-order structure \mathcal{H} .

The processing stages of our method are summarized in Figure 1. First, we will predict the latent hypergraph based on the input features \mathbf{X} . The inferred hypergraph structure will then be fed into a hypergraph network to obtain the final prediction. To obtain a powerful, general model, our method needs to fulfill two important characteristics. Firstly, the entire pipeline need to be end-to-end differentiable, such that the latent hypergraph inference can be trained in a weakly supervised fashion, solely from the final downstream prediction, without access to the ground-truth hypergraph structure. Secondly, the model needs to be general enough such that it can be used inside any existing architecture for hypergraph processing.

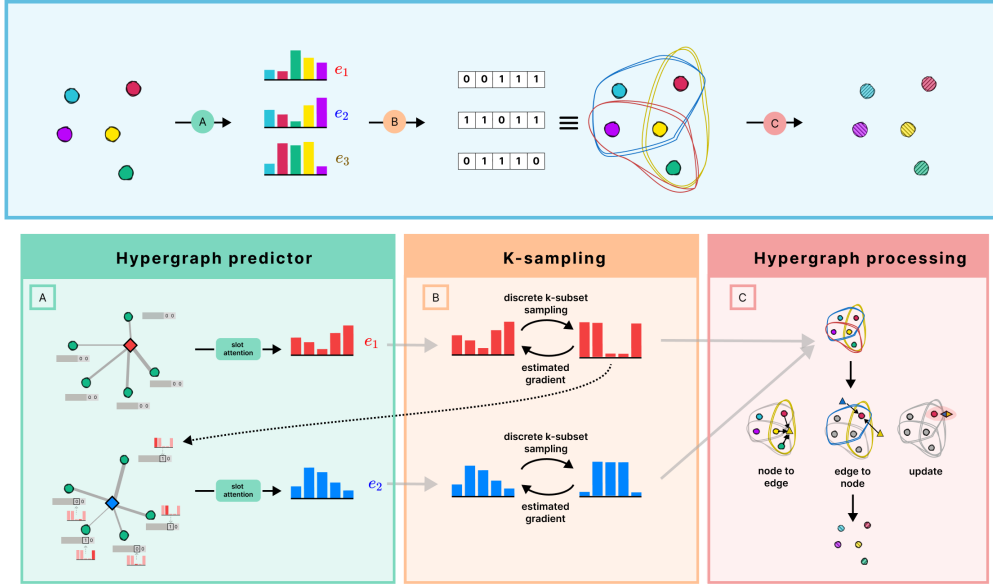


Figure 1: **SPHINX architecture**, designed to capture higher-order interactions without having access to the ground-truth hypergraph structure. The model consists of three stages: A) The **hypergraph predictor** infers a probabilistic latent hypergraph structure, by using a sequential clustering algorithm to produce global, history-aware hyperedges. At each timestep, the node features are enriched with the information about the already predicted hyperedges and the resulting cluster represent the hyperedge membership. B) A **k -subset sampling** algorithm is applied to transform each probability distribution into discrete incidence relations, while maintaining the end-to-end differentiability of the framework. The k -nodes constraint ensures a more stable optimisation process, beneficial for the final performance. C) The predicted hypergraph structure can be used in any standard **hypergraph neural network** in order to produce higher-order representations.

To achieve these desiderata, we designed the model using two core components: a learnable soft clustering that predicts a probability distributions for each one of the M potential hyperedges, and a differentiable k -sampling that, based on these probability distribution, samples discrete subsets of k nodes forming the hypergraph structure. Both components are differentiable such that the model can be easily trained using standard backpropagation techniques. Moreover, the predicted hypergraph structure is a discrete object, following the classical structural representation used in any hypergraph processing models $\mathcal{H} = (V, E)$, where V is a the of nodes and E is a the of hyperedges.

3.1 Hypergraph predictor

The goal of this module is to transform a set of node features $\mathbf{X} \in \mathbb{R}^{N \times f}$ into a set of incidence probabilities $\mathbf{P} \in \mathbb{R}^{N \times M}$ where N represents the number of node and M represents the expected number of hyperedges. Each column $j \in \{1 \dots M\}$ corresponds to a hyperedge and represents the probability of each node being part of the hyperedge j . In order to accurately predict these probabilities, the model needs to have a global understanding of the nodes interactions and identify the subsets that are more likely to exhibit a higher-order relationship.

Taking inspiration from the computer vision literature for unsupervised object detection [44], we model the hypergraph discovery task as a soft clustering problem, where each cluster correspond to a hyperedge. We adapt the iterative slot-attention algorithm [45] to produce M clusters, each one corresponding to a predicted hyperedge. The probability of a node i being part of a cluster j , computed as the node-cluster similarity, represents the incidence probabilities p_{ij} corresponding to node i and hyperedge j . Therefore, we will use the terms slots and hyperedges interchangeably.

Slot Attention for probabilistic incidence prediction. We start by creating M slots, one for each hyperedge. Each slot $s_j \in \mathbb{R}^f$ is randomly initialized from a normal distribution. At each iteration, the

slots representation is updated as the weighted average of all the nodes, with the weights computed as a learnable dot-product similarity as indicated by Equation 1, where f_1 , f_2 and f_3 represent MLPs and σ is a non-linearity. After Q iterations, the pairwise similarity between the updated slot representation and the set of node features represents the predicted probability distribution $p_{:,j}$ for hyperedge j .

$$s_j^{q+1} = \sum_i (\sigma(f_1(s_j^q)^T f_2(x_i)) f_3(x_i)) \quad (1)$$

$$p_{i,j} = p(v_i \in e_j) = \sigma(f_1(s_j^Q)^T f_2(x_i)) \quad (2)$$

Note that this procedure is similar to a differentiable k -means clusterization, where the hyperedges represent the centroids and the similarity coefficient represent the soft assignment corresponding to each node-cluster pair. At a high level, the probability of a node being part of a hyperedge can be interpreted as the likelihood of an element being assigned to a certain cluster.

Sequential Slot Attention for solving ambiguities. The above algorithm suffers from a strong limitation. Due to the symmetries exhibited by the set of hyperedges, independently inferring M hyperedges leads to strong ambiguity issues. Concretely, since the slots are initialized randomly, there is no mechanism in place to distribute the hyperedges between slots: multiple slots could be attached to the same obvious hyperedge, leaving others completely uncovered.

To alleviate this, we propose a sequential slot attention. Instead of predicting all hyperedges simultaneously, we will predict them sequentially, one at a time, ensuring that at each timestep the hyperedge prediction mechanism is aware of the hyperedges predicted so far. To achieve that, the features of each node x_i is enriched with an additional binary vector $b_i \in \{0, 1\}^{(M-1)}$ indicating the relationship between that node and the previously predicted hypergraphs. Specifically, when predicting hyperedge j , for each previous hyperedge t ($t < j$), $b_{it} = 1$ if the node i was previously selected to be part of the hyperedge t and $b_{it} = 0$ otherwise. This way, the slot-attention algorithm has the capacity to produce more diverse hyperedges, as we experimentally validated in Section 4.1.

3.2 Discrete constrained sampling

The hypergraph predictor module, as described above, produces a probabilistic incidence matrix $\mathbf{P} \in \mathbb{R}^{N \times M}$, where each element $p_{i,j}$ denotes the probability of a node i being part of the hyperedge j . However, the standard hypergraph neural network architectures are designed to work with discrete rather than probabilistic structures.

Previous work [43] employs Gumbel-Softmax [10] to sample from a categorical distribution in a differentiable way. However, these techniques sample each element in the hyperedge independently, without any control on the cardinality of the hyperedge. This leads to unstable optimisation, that requires additional training strategies such as specific sparsity regularisation.

To address this issue, we are leveraging the recent advancement in constrained k -subset sampling [8, 46, 9]. These methods were successfully used to tackle discrete problems such as combinatorial optimisation, learning explanations and, more recently, rewiring graph topology [47]. Different than classical differentiable samplers [10], the k -subset sampler would produce a subset of size exactly k , equipped with a gradient estimator useful for backpropagation.

In our work, we took advantage of these recent advancements and apply it to produce a discrete incidence matrix from the probabilities inferred by the slot attention algorithm. Concretely, given the probability distribution $p_{:,j}$ for each hyperedge j , the discrete sampler would select a subset of nodes, representing the group of nodes forming the hyperedge. As demonstrated in Section 4.1, by ensuring that each hyperedge contains exactly k elements, this approach improves over the previous techniques, manifesting an easier optimisation. While the cardinality k needs to be set apriori, as a hyperparameter, this value can vary between different hyperedges.

3.3 Hypergraph processing

Producing a discrete hypergraph structure and being able to propagate the gradient through the entire pipeline, enable us to process the resulting latent hypergraph with any existing architecture designed for higher-order representations. In the recent years, several architectures were developed for hypergraph-structured input [26, 48, 27, 28]. Most of them are following the general two-stage

message-passing framework. In the first stage, the information is sent from nodes to the hyperedges using a permutation-invariant operator $z_j = f_{V \rightarrow E}(\{x_i | v_i \in e_j\})$. On the second stage the messages are sent back from hyperedge to nodes $x_i = f_{E \rightarrow V}(\{z_j | v_i \in e_j\})$.

In our experiments we use a similar setup to the one proposed in [28], in which the two functions $f_{V \rightarrow E}$ and $f_{E \rightarrow V}$ are implemented as DeepSets [29] models.

$$f_{V \rightarrow E}(S) = f_{E \rightarrow V}(S) = \text{MLP}\left(\sum_{s \in S} (\text{MLP}(s))\right)$$

Note that, although we experimented primarily with the architecture presented above, the framework is general enough to be used with any other hypergraph network. Our experiments demonstrated that even simpler hypergraph models enable the discovery of accurate higher-order structures.

4 Experimental Analysis

While the importance of higher-order processing is widely accepted in the machine learning community [49] and beyond [50], the amount of benchmarks developed to properly validate the hypergraph methods is still insufficient. This issue becomes even more pronounced when it comes to latent hypergraph inference. Although there is evidence that many existing real-world tasks exhibit underlining higher-order interactions that can be beneficial to capture, evaluating the capability of a neural network to predict the latent structure remains challenging. First, the input features should contain enough information to predict the hypergraph structure. Secondly, even if we do not need the hypergraph structure as a supervision signal, having access to it is necessary to properly evaluate to what extent the model learns to infer the correct structure.

To alleviate these shortcomings, current works adopt one of the following approaches: either using synthetic data, where we can directly have access to the higher-order relationships used to generate the outcome, or by using real-world data and only evaluate the capability of the model to improve the final prediction, without directly computing the accuracy of the discovered latent structure.

In our work we adopt both of these approaches. First, we will perform an in depth ablation study on a synthetic dataset containing particle simulations. Then, we will move on to the NBA real-world dataset where we will evaluate to what extent our latent hypergraph structure improves the trajectory prediction performance. Our goal is two fold. We show that our model is capable of learning an appropriate latent hypergraph structure in an unsupervised way. Additionally, we prove that the latent higher-order structure, learnt jointly with the rest of the model, helps the performance of the downstream task.

4.1 Particle Simulations

Our simulated system consist of N particles moving in a 2D space. For each example, K random triangles were uniformly sampled to represent K 3-order interactions. All the particles that are part of a triangle rotate around the triangle’s center of mass with a random angular velocity θ_i characteristic to each particle i . If one particle is part of multiple triangles, the rotation will happen around their average center of mass. Examples of such trajectories are depicted in Figure 3. For each trajectory we observe the position of the particles in the first 22 steps, and the task is to infer the trajectory for the following 25 steps. We are experimenting with 2 variants of the dataset. A simpler one, containing a single higher-order interaction per trajectory (denoted as One-Triangle), and a more challenging one containing two higher-order interaction per trajectory (denoted as Two-Triangles). Each dataset contains 1000 training, 1000 validation and 1000 test trajectories.

For all our experiments, the hypergraph predictor treats particles as nodes. For each particle, the node features consist of the (x, y) coordinates corresponding to the first T timesteps. These features will be used to predict the hypergraph incidence matrix H . During training, the hypergraph processor receives the predicted hypergraph structure together with the particle’s position at timestep t , and the goal is to predict the position of the particles at timestep $t + 1$. To generate longer trajectories, during testing, the model receives at each moment in time the position predicted at the previous timestep.

Hypergraph discovery. These datasets allow us to experiment with learning the higher-order relations in a setup where we have access to the ground-truth connectivity. Our model produces discrete hypergraph structures that we can inspect and evaluate, offering an additional level of

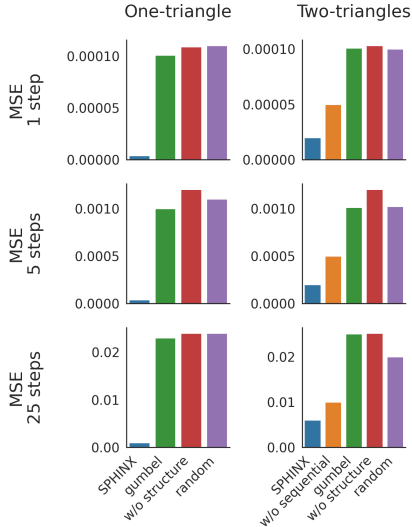


Figure 2: **Ablation studying the importance of hypergraph inference** on the Particle Simulation. The sequential prediction and constrained k -subset sampling clearly helps the performance. SPHINX obtains the best results across both datasets.

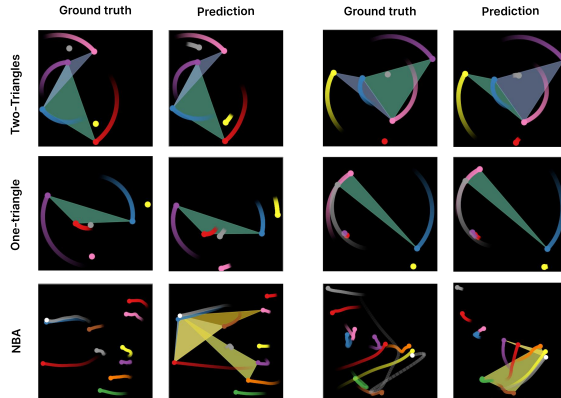


Figure 3: **Predicted trajectories and the latent hypergraph structures** on the Particle Simulation and the real-world NBA datasets. The model learns to produce accurate trajectories and useful hypergraph structures (depicted as polygons) that correlates well with the ground truth connectivity. We observe that, for the NBA dataset, the hyperedges tends to contain the ball-node (represented as a white dot). This aligns well with our intuition that players dynamics should be highly influence by the position of the ball.

interpretability to the framework. Visualisations of our learned hypergraph structure (see Figure 3) reveals that they are highly correlated to the ground-truth interactions used to generate the dataset.

We quantitatively evaluate to what extent our model learns the true higher-order relationships, by computing the overlap between our model’s prediction and the ground-truth hyperedges. We refer to the Supplementary Material for a full descriptions of the metric used in this experiments. In Figure 4 we observe that, even if we do not explicitly optimise for this task, the accuracy of the hypergraph structure predictor increases during training, reaching more than 90% overlap for both the One-Triangle dataset and the Two-Triangles dataset.

General and versatile, our model is designed to predict hypergraph structure that is useful for any hypergraph neural network. However, since the supervision signal comes from the high-level tasks, the architecture used for hypergraph processing can impose certain inductive biases, influencing the hypergraph structure learned by the predictor. In the experiment depicted in Figure 4, we investigate to what extent our model learns an accurate higher-order structure, regardless of the hypergraph processing architecture. We train a set of models using the same hypergraph predictor for inferring the hypergraph structure, but various hypergraph networks for processing it. For this, we experiment with AllDeepSets [28], HGNN [26] and HCHA [31]. The results show that our model is capable of learning the suitable structure irrespective of the specifics in the processing model.

These experiments prove that the hypergraph discovery task is highly correlated with the trajectory prediction problem. Our model, explicitly designed to infer the latent hypergraph structure, is capable not only to accurately solve the downstream task but also to recover the true higher-order relations, without access to the ground-truth hypergraph connectivity.

Importance of sequential prediction. While the classical slot-attention algorithm infers all the clusters in parallel, we argue that this is not an appropriate design choice for hypergraph prediction. Often, the set of hyperedges is mostly symmetric, which makes the problem of attaching the slots to different hyperedges highly ambiguous. In fact, we visually observed that, when predicting all the hyperedges simultaneously, the model tends to associate multiple slots to the same hyperedge, leaving others completely uncovered (see Supplementary Material for more visualisations). This behaviour leads to both a decrease in downstream performance and a less accurate hypergraph predictor. As described in Section 3.1, SPHINX alleviates this issue by inferring the slots sequentially, and providing at each step historical information about the structure predicted so far. Figure 2 and

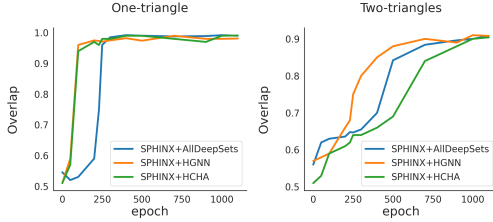


Figure 4: **Hypergraph discovery improves during training** on the synthetic datasets, even if the model is not supervised for this task. Regardless of the hypergraph architectures, the overlap between our (unsupervised) predicted hypergraph and the gt. connectivity increases, demonstrating that the model recovers the real structure to a high extent.

Table 1: **Ablation study on the NBA dataset.** Both using sequential, history-aware predictors and using k -subset sampling prove to be beneficial for the final performance (ADE/FDE metrics reported). Moreover, our model shows a clear advantage compared to the best recent work on the single-trajectory prediction task.

Time	GroupNet	SPHINX w/o sequential	SPHINX w Gumbel	SPHINX
1sec	0.65/1.03	0.62/0.94	1.29/1.81	0.59/0.92
2sec	1.38/2.61	1.18/2.08	2.10/3.34	1.12/2.06
3sec	2.15/4.11	1.73/3.14	2.81/4.60	1.65/3.13
4sec	2.83/5.15	2.25/4.08	3.45/5.66	2.14/4.09

Table 1 demonstrates the benefits of our design choices. Sequential prediction have a clear advantage, outperforming the classical slot-attention predictor.

Influence of k -sampling. Previous work on inferring hypergraphs [43] takes inspiration from the graph relational inference [19] where the differentiable sampling is achieved using the Gumbel-Softmax trick. We argue that, inferring the subset of nodes that are part of a hyperedge generates more challenges compare to the graph scenarios. In the beginning of training, sampling each node-hyperedge incidence independently, without any constraints, can lead to hyperedges containing either too few or too many nodes, which highly damage the optimisation. In this work, we leverage the recent advance in differentiable k -subset sampling, which imposes the k -nodes constraint, while still allowing to estimate the gradient during backpropagation. The experiments in Figure 2 show that the k -subset sampling improves the results, leading to an easier optimisation and better final performance. This is in line with the results reported in [43] where smoothness and sparsity regularisation are crucial for improving the results on a real-world dataset. In contrast, our model obtains competitive performance without any optimisation trick.

Comparison with baselines. Both versions of the datasets used in our experiments heavily relies on higher-order processing. In order to predict the particle movement, the model needs to identify the higher-order structures that guides the rotation and use it to generate the displacement from the previous position. To understand to what extent our model is able to produce and process a useful hypergraph structure, we compare against two baseline: a model using a random structure (denoted as *random* in Figure 2) and a node-level model, that ignores the hypergraph structure (denoted as *w/o structure*) by setting the incidence matrix on zero. Both models perform much worse than our learnable hypergraph model, indicating that the dataset highly depends on higher-order interactions and our model is capable of discovering an appropriate latent structure. Inspired by [19], we also compare our model against an LSTM baseline that is agnostic to the hypergraph structure and only receives the concatenation of all the particles. While performing comparable on the 1 step prediction metric ($2e-5$ MSE for SPHINX and $3e-5$ for the LSTM), the performance degrades quickly when evaluating on the long-range prediction ($6e-3$ MSE for SPHINX compared to $1.7e-1$ for the LSTM). For the complete numerical results, see Supplementary Material.

Implementation details. Unless otherwise stated, the One-Triangle experiments use a single slot in the slot-attention module, while the Two-Triangles uses two slots. For estimating the gradients in the k -subset sampling algorithm we experiment with SIMPLE [8], AIMLE [9] and IMLE [46] algorithms. According to our experiments, the first two perform on par, while IMLE [46] mostly suffer from gradient issues. Unless otherwise specified, our models use the AllDeepSets [28] hypergraph processor. In all experiments, we use Adam optimizer for 1000 epochs, trained on a single GPU.

Key findings. The results presented in this section demonstrates that: ① Our model predicts accurate hypergraph connectivity, that correlates well with the ground-truth structure, even without being optimized for this task and ② irrespective of the hypergraph architecture used as decoder. ③ Predicting the hyperedges sequentially ameliorate the ambiguity issue, improving the hypergraph inference. ④ k -subset sampling is crucial for a good performance, proving to be superior to the standard Gumbel-Softmax approach and allows us to eliminate the regularisation tricks. ⑤ Finally, discovering the latent hypergraph structure is clearly beneficial for the downstream prediction.

Table 2: **Performance on the NBA dataset** in terms of minADE_{20} and minFDE_{20} metrics. Our model performing higher-order processing using a learnable hypergraph structure prove to be beneficial for trajectory prediction tasks, obtaining competitive performance.

Time	NRI	DNRI	EvolveGraph	STGAT	Trajectron++	EvolveHgraph HO only	EvolveHgraph full	GroupNet	SPHINX
1sec	0.51/0.74	0.59/0.70	0.35/0.48	0.45/0.66	0.44/0.67	0.49/0.74	0.33/0.49	0.34/0.48	0.30/0.43
2sec	0.96/1.65	0.93/1.52	0.66/0.97	0.87/1.41	0.79/1.18	0.95/1.68	0.63/0.95	0.62/0.95	0.59/0.94
3sec	1.42/2.50	1.38/2.21	1.15/1.86	1.28/2.08	1.51/2.49	1.44/2.27	0.93/1.36	0.87/1.31	0.88/1.38
4sec	1.86/3.26	1.78/2.81	1.64/2.64	1.69/2.66	2.09/3.52	1.91/3.08	1.21/1.74	1.13/1.69	1.16/1.74

4.2 NBA Dataset

To evaluate our model on a real-world dataset, we use the NBA SportVU dataset, containing information about the movement of the players during the basketball matches. Each example contains 11 trajectories, 5 players from each team and one trajectory for the ball. Similar to the synthetic setup, the hypergraph predictor receives as node features the first part of each trajectory (the initial 5 steps) and the goal is to predict the next 10 steps. While our model is not especially designed as a tracking systems, the dynamics followed by the basketball game contains higher-order relations that are difficult to identify, thus representing a good testbed for our hypergraph inference method.

Ablation study. We assess our core design choices on the real-world dataset as well. In Table 1 we are reporting the average displacement error (ADE) and final displacement error (FDE) metrics. Similar to the particle simulation datasets, we observe that predicting the hyperedges sequentially outperforms the simultaneous approach used by standard differentiable clustering algorithms. Moreover, the k -subset sampling prove to be clearly superior to the Gumbel-Softmax used in the previous methods.

Comparison to recent methods. In Table 2 we compare against other structure-based methods in the literature including graph-based methods: NRI [19], DNRI [22], EvolveGraph [51], STGAT [52], Trajectron++ [53] and hypergraph-based methods: higher-order-only EvolveHypergraph, the full EvolveHypergraph model [43] and GroupNet [42]. Our method improves the short and medium-term prediction, while obtaining competitive results on the long-term prediction. Note that, compared to the other hypergraph-based methods, our model do not requires any auxiliary loss function or additional pairwise predictions.

The metrics used in the recent literature (minADE_{20} and minFDE_{20}) takes into account only the best trajectory from a pool of 20 sampled trajectories. Recent work [54] shows that these metrics suffer from a series of limitations, favouring methods that produce diverse, but not necessarily accurate trajectories. Thus, in Table 1, we also compared against the top hypergraph-based method using the single-trajectory prediction metrics, ADE and FDE (the code for EvolveHypergraph is not publicly available). The results clearly show that for single-trajectory prediction our method obtains better results both on short and long-term prediction.

Implementation details. In all our experiments we follow the train-valid-test split from [42]. For the observed trajectory, besides the coordinates of each player, the node features are enhanced with the velocity computed based on consecutive frames. For the unobserved trajectory, the velocity is computed based on the predicted position. The models are trained for 300 epochs, using Adam optimiser with learning rate 0.001, decreased by a factor of 10 when reaching a plateau. Similar to the synthetic setup, we are treating the algorithm used to perform k -sampling as a hyperparameter, experimenting with both AIMLE [9] and SIMPLE [8] algorithm. More details for the hyperparameters tuned in our experiments are presented in the Supplementary Material.

5 Conclusion

In this paper we are introducing Structural Prediction using Hypergraph Inference Network (SPHINX), a model for unsupervised hypergraph inference that enables higher-order processing in tasks where hypergraph structure is not provided. The model adopts a global processing in the form of sequential soft clustering for predicting hyperedge probability, paired with a k -subset sampling algorithm for discretizing the structure such that it can be used with any hypergraph neural network decoder and eliminating the need for heavy optimisation tricks. Overall, the resulting method is a general and broadly applicable solution for relational processing, facilitating seamless integration into any real-world systems perceived to necessitate higher-order analysis.

Acknowledgment The authors would like to thank Charlotte Magister, Daniel McFadyen, Alex Norcliffe and Paul Scherer for fruitful discussions and constructive suggestions during the development of the paper. Iulia Duta is a PhD student funded by a Twitter scholarship.

References

- [1] Nicolas A. Crossley, Andrea Mechelli, Jessica Scott, Francesco Carletti, Peter T. Fox, Philip K. McGuire, and Edward T. Bullmore. The hubs of the human connectome are generally implicated in the anatomy of brain disorders. *Brain*, 137:2382 – 2395, 2014.
- [2] Tingting Guo, Yining Zhang, Yanfang Xue, and Lishan Qiao. Brain function network: Higher order vs. more discrimination. *Frontiers in Neuroscience*, 15, 08 2021.
- [3] Jürgen Jost and Raffaella Mulas. Hypergraph laplace operators for chemical reaction networks, 2018.
- [4] Ramon Viñas, Chaitanya K. Joshi, Dobrik Georgiev, Bianca Dumitrascu, Eric R. Gamazon, and Pietro Liò. Hypergraph factorisation for multi-tissue gene expression imputation. *bioRxiv*, 2022.
- [5] Jure Leskovec, Jon M. Kleinberg, and Christos Faloutsos. Graphs over time: densification laws, shrinking diameters and possible explanations. In *Knowledge Discovery and Data Mining*, 2005.
- [6] Weihua Hu, Matthias Fey, Marinka Zitnik, Yuxiao Dong, Hongyu Ren, Bowen Liu, Michele Catasta, and Jure Leskovec. Open graph benchmark: Datasets for machine learning on graphs. In H. Larochelle, M. Ranzato, R. Hadsell, M.F. Balcan, and H. Lin, editors, *Advances in Neural Information Processing Systems*, volume 33, pages 22118–22133. Curran Associates, Inc., 2020.
- [7] Yanbang Wang and Jon Kleinberg. From graphs to hypergraphs: Hypergraph projection and its reconstruction. In *The Twelfth International Conference on Learning Representations*, 2024.
- [8] Kareem Ahmed, Zhe Zeng, Mathias Niepert, and Guy Van den Broeck. Simple: A gradient estimator for k-subset sampling. In *Proceedings of the International Conference on Learning Representations (ICLR)*, may 2023.
- [9] Pasquale Minervini, Luca Franceschi, and Mathias Niepert. Adaptive perturbation-based gradient estimation for discrete latent variable models. *Proceedings of the AAAI Conference on Artificial Intelligence*, 37(8):9200–9208, Jun. 2023.
- [10] Eric Jang, Shixiang Gu, and Ben Poole. Categorical reparameterization with gumbel-softmax. In *5th International Conference on Learning Representations, ICLR 2017, Toulon, France, April 24-26, 2017, Conference Track Proceedings*. OpenReview.net, 2017.
- [11] Thomas N. Kipf and Max Welling. Semi-supervised classification with graph convolutional networks. In *International Conference on Learning Representations (ICLR)*, 2017.
- [12] Petar Veličković, Guillem Cucurull, Arantxa Casanova, Adriana Romero, Pietro Liò, and Yoshua Bengio. Graph attention networks. In *International Conference on Learning Representations*, 2018.
- [13] Ioana Bica and Mihaela van der Schaar. Transfer learning on heterogeneous feature spaces for treatment effects estimation. In S. Koyejo, S. Mohamed, A. Agarwal, D. Belgrave, K. Cho, and A. Oh, editors, *Advances in Neural Information Processing Systems*, volume 35, pages 37184–37198. Curran Associates, Inc., 2022.
- [14] Alvaro Sanchez-Gonzalez, Jonathan Godwin, Tobias Pfaff, Rex Ying, Jure Leskovec, and Peter Battaglia. Learning to simulate complex physics with graph networks. In Hal Daumé III and Aarti Singh, editors, *Proceedings of the 37th International Conference on Machine Learning*, volume 119, pages 8459–8468, 2020.

- [15] Remi Lam, Alvaro Sanchez-Gonzalez, Matthew Willson, Peter Wirsberger, Meire Fortunato, Ferran Alet, Suman Ravuri, Timo Ewalds, Zach Eaton-Rosen, Weihua Hu, Alexander Merose, Stephan Hoyer, George Holland, Oriol Vinyals, Jacklynn Stott, Alexander Pritzel, Shakir Mohamed, and Peter Battaglia. Learning skillful medium-range global weather forecasting. *Science*, 382(6677):1416–1421, 2023.
- [16] Alex Davies, Petar Velickovic, Lars Buesing, Sam Blackwell, Daniel Zheng, Nenad Tomasev, Richard Tanburn, Peter W. Battaglia, Charles Blundell, András Juhász, Marc Lackenby, Geordie Williamson, Demis Hassabis, and Pushmeet Kohli. Advancing mathematics by guiding human intuition with ai. *Nature*, 600:70 – 74, 2021.
- [17] Zhe Wang, Petar Veličković, Daniel Hennes, Nenad Tomašev, Laurel Prince, Michael Kaisers, Yoram Bachrach, Romuald Elie, Li Wenliang, Federico Piccinini, William Spearman, Ian Graham, Jerome Connor, Yi Yang, Adrià Recasens, Mina Khan, Nathalie Beauguerlange, Pablo Sprechmann, Pol Moreno, and Karl Tuyls. Tacticai: an ai assistant for football tactics. *Nature Communications*, 15, 03 2024.
- [18] Justin Gilmer, Samuel S. Schoenholz, Patrick F. Riley, Oriol Vinyals, and George E. Dahl. Neural message passing for quantum chemistry. In Doina Precup and Yee Whye Teh, editors, *Proceedings of the 34th International Conference on Machine Learning*, volume 70 of *Proceedings of Machine Learning Research*, pages 1263–1272, 2017.
- [19] T. Fetaya, Elias Wang, K.-C. Welling, Michelle Zemel, Thomas Kipf, Ethan Fetaya, Kuan-Chieh Jackson Wang, Max Welling, and Richard S. Zemel. Neural relational inference for interacting systems. In *International Conference on Machine Learning*, 2018.
- [20] Ezra Webb, Ben Day, Helena Andrés-Terré, and Pietro Lio’. Factorised neural relational inference for multi-interaction systems. *ArXiv*, abs/1905.08721, 2019.
- [21] Sindy Lowe, David Madras, Richard Zemel, and Max Welling. Amortized causal discovery: Learning to infer causal graphs from time-series data. *Causal Learning and Reasoning (CLEaR)*, 2022.
- [22] Colin Graber and Alexander G. Schwing. Dynamic neural relational inference. In *Proceedings of the IEEE/CVF Conference on Computer Vision and Pattern Recognition (CVPR)*, June 2020.
- [23] Joaquín J. Torres and Ginestra Bianconi. Simplicial complexes: higher-order spectral dimension and dynamics. *Journal of Physics: Complexity*, 1, 2020.
- [24] Albert T. Lundell and Stephen Weingram. *CW Complexes*, pages 41–76. Springer New York, New York, NY, 1969.
- [25] Anirban Banerjee. On the spectrum of hypergraphs. *Linear Algebra and its Applications*, 614:82–110, 2021. Special Issue ILAS 2019.
- [26] Yifan Feng, Haoxuan You, Zizhao Zhang, Rongrong Ji, and Yue Gao. Hypergraph neural networks. *Proc. Conf. AAAI Artif. Intell.*, 33(01):3558–3565, July 2019.
- [27] Jing Huang and Jie Yang. Unignn: a unified framework for graph and hypergraph neural networks. In *Proceedings of the Thirtieth International Joint Conference on Artificial Intelligence, IJCAI-21*, 2021.
- [28] Eli Chien, Chao Pan, Jianhao Peng, and Olgica Milenkovic. You are allset: A multiset function framework for hypergraph neural networks. In *International Conference on Learning Representations*, 2022.
- [29] Manzil Zaheer, Satwik Kottur, Siamak Ravanbakhsh, Barnabas Poczos, Russ R Salakhutdinov, and Alexander J Smola. Deep sets. In I. Guyon, U. Von Luxburg, S. Bengio, H. Wallach, R. Fergus, S. Vishwanathan, and R. Garnett, editors, *Advances in Neural Information Processing Systems*, volume 30. Curran Associates, Inc., 2017.
- [30] Ashish Vaswani, Noam Shazeer, Niki Parmar, Jakob Uszkoreit, Llion Jones, Aidan N Gomez, Łukasz Kaiser, and Illia Polosukhin. Attention is all you need. In I. Guyon, U. Von Luxburg, S. Bengio, H. Wallach, R. Fergus, S. Vishwanathan, and R. Garnett, editors, *Advances in Neural Information Processing Systems*, volume 30. Curran Associates, Inc., 2017.

- [31] Song Bai, Feihu Zhang, and Philip H.S. Torr. Hypergraph convolution and hypergraph attention. *Pattern Recognition*, 110:107637, 2021.
- [32] Jiying Zhang, Yuzhao Chen, Xiong Xiao, Runiu Lu, and Shutao Xia. Learnable hypergraph laplacian for hypergraph learning. In *ICASSP*, 2022.
- [33] Dobrik Georgiev Georgiev, Marc Brockschmidt, and Miltiadis Allamanis. HEAT: Hyperedge attention networks. *Transactions on Machine Learning Research*, 2022.
- [34] Iulia Duta, Giulia Cassarà, Fabrizio Silvestri, and Pietro Lio. Sheaf hypergraph networks. In *Thirty-seventh Conference on Neural Information Processing Systems*, 2023.
- [35] Hypergraph reconstruction from network data. *Communications Physics*, 4(1), June 2021.
- [36] Detecting informative higher-order interactions in statistically validated hypergraphs. *Communications Physics*, 4, 2021.
- [37] Claudio Battiloro, Indro Spinelli, Lev Telyatnikov, Michael M. Bronstein, Simone Scardapane, and Paolo Di Lorenzo. From latent graph to latent topology inference: Differentiable cell complex module. *ArXiv*, abs/2305.16174, 2023.
- [38] David W Zhang, Gertjan J. Burghouts, and Cees G. M. Snoek. Pruning edges and gradients to learn hypergraphs from larger sets. In Bastian Rieck and Razvan Pascanu, editors, *Proceedings of the First Learning on Graphs Conference*, volume 198 of *Proceedings of Machine Learning Research*, pages 53:1–53:18. PMLR, 09–12 Dec 2022.
- [39] Jun Yu, Dacheng Tao, and Meng Wang. Adaptive hypergraph learning and its application in image classification. *IEEE Transactions on Image Processing*, 21(7):3262–3272, 2012.
- [40] Zizhao Zhang, Haojie Lin, and Yue Gao. Dynamic hypergraph structure learning. *IJCAI’18*, page 3162–3169. AAAI Press, 2018.
- [41] Yue Gao, Zizhao Zhang, Haojie Lin, Xibin Zhao, S. Du, and Changqing Zou. Hypergraph learning: Methods and practices. *IEEE Transactions on Pattern Analysis and Machine Intelligence*, 44:2548–2566, 2020.
- [42] Chenxin Xu, Maosen Li, Zhenyang Ni, Ya Zhang, and Siheng Chen. Groupnet: Multiscale hypergraph neural networks for trajectory prediction with relational reasoning. In *The IEEE/CVF Conference on Computer Vision and Pattern Recognition (CVPR)*, 2022.
- [43] Jiachen Li, Chuanbo Hua, Jinkyoo Park, Hengbo Ma, Victoria Dax, and Mykel J. Kochenderfer. Evolvehypergraph: Group-aware dynamic relational reasoning for trajectory prediction, 2022.
- [44] Klaus Greff, Sjoerd van Steenkiste, and Jürgen Schmidhuber. On the binding problem in artificial neural networks. *ArXiv*, abs/2012.05208, 2020.
- [45] Francesco Locatello, Dirk Weissenborn, Thomas Unterthiner, Aravindh Mahendran, Georg Heigold, Jakob Uszkoreit, Alexey Dosovitskiy, and Thomas Kipf. Object-centric learning with slot attention. *arXiv preprint arXiv:2006.15055*, 2020.
- [46] Mathias Niepert, Pasquale Minervini, and Luca Franceschi. Implicit MLE: Backpropagating through discrete exponential family distributions. In A. Beygelzimer, Y. Dauphin, P. Liang, and J. Wortman Vaughan, editors, *Advances in Neural Information Processing Systems*, 2021.
- [47] Chendi Qian, Andrei Manolache, Kareem Ahmed, Zhe Zeng, Guy Van den Broeck, Mathias Niepert, and Christopher Morris. Probabilistically rewired message-passing neural networks. *ArXiv*, abs/2310.02156, 2023.
- [48] Peihao Wang, Shenghao Yang, Yunyu Liu, Zhangyang Wang, and Pan Li. Equivariant hypergraph diffusion neural operators. *arXiv preprint arXiv:2207.06680*, 2022.
- [49] Dengyong Zhou, Jiayuan Huang, and Bernhard Schölkopf. Learning with hypergraphs: Clustering, classification, and embedding. In B. Schölkopf, J. Platt, and T. Hoffman, editors, *Advances in Neural Information Processing Systems*, volume 19. MIT Press, 2006.

- [50] Songyang Zhang, Zhi Ding, and Shuguang Cui. Introducing hypergraph signal processing: Theoretical foundation and practical applications. *IEEE Internet of Things Journal*, 7(1):639–660, 2020.
- [51] Jiachen Li, Fan Yang, Masayoshi Tomizuka, and Chiho Choi. Evolvegraph: Multi-agent trajectory prediction with dynamic relational reasoning. *arXiv: Computer Vision and Pattern Recognition*, 2020.
- [52] Yingfan Huang, Huikun Bi, Zhaoxin Li, Tianlu Mao, and Zhaoqi Wang. Stgat: Modeling spatial-temporal interactions for human trajectory prediction. *2019 IEEE/CVF International Conference on Computer Vision (ICCV)*, pages 6271–6280, 2019.
- [53] Tim Salzmann, Boris Ivanovic, Punarjay Chakravarty, and Marco Pavone. Trajectron++: Dynamically-feasible trajectory forecasting with heterogeneous data. In *Computer Vision – ECCV 2020: 16th European Conference, Glasgow, UK, August 23–28, 2020, Proceedings, Part XVIII*, page 683–700, Berlin, Heidelberg, 2020. Springer-Verlag.
- [54] Ross Greer, Nachiket Deo, and Mohan Manubhai Trivedi. Trajectory prediction in autonomous driving with a lane heading auxiliary loss. *IEEE Robotics and Automation Letters*, 6:4907–4914, 2020.
- [55] Sepp Hochreiter and Jürgen Schmidhuber. Long short-term memory. *Neural computation*, 9(8):1735–1780, 1997.

Appendix: SPHINX Structural Prediction using Hypergraph Inference Network

This appendix contains details related to our proposed Structural Prediction using Hypergraph Inference Network (SPHINX) model, including broader impact and potential limitations, qualitative visualisations from our model and the baselines we compared against in this paper, details about the proposed dataset, information about the implementation of the model and additional experiments referred in the main paper.

- **Section A** highlights a series of potential limitations that can be address to improve the current work, together with a discussion about the social impact of our approach.
- **Section B** contains visualisation of the discovered hypergraph structure and the predicted trajectory for our proposed model and different variations of it.
- **Section C** provides more details about the proposed synthetic dataset, further information about the method and its training process.
- **Section D** presents additional ablation studies showing the influence of varying the number of hyperedges in our model, but also a more detailed analysis of the synthetic experiments presented in the paper, including the numerical results.

A Broader Impact & Limitations

In this paper, we are proposing a framework for processing higher-order interactions in scenarios where a ground-truth hypergraph connectivity is either too expensive or not accessible at all. We are showing that our model is capable of recovering the latent higher-order structure without supervision at the hypergraph level, thus improving the final, higher-level performance. While we mainly tested on trajectory prediction tasks, our model is general and versatile and can be applied to any scenarios where we suspect capturing and modeling higher-order relations can be beneficial. Consequently, we believe that our model doesn't have any direct negative societal impact. Moreover, the method has the advantage of allowing us to inspect the learned latent hypergraph structure (as we can see in Section B of this Supplementary Material). This offer an advantage in terms of interpretability, allowing us to better understand and address potential mistakes in the model's prediction.

By construction, our model predicts a set of M slots, each one corresponding to a hyperedge. This process is sequential, with one slot predicted at each time-step. While stopping criterion can be imposed to allow dynamic number of hyperedges, in order to be able to take advantage of the historical features $b \in \{0, 1\}^{N \times (M-1)}$ we need to have access to a pre-defined maximum number of hyperedges M . In the current version of our work, this number is picked as a hyperparameter. However, in Section D, we experimentally show that the chosen value doesn't have a significant impact on the results. As long as the number of hyperedges is larger than the expected one, the performance doesn't decrease.

Furthermore, as we show in our experimental analysis, the k -subset sampling has a clear, positive impact on the performance of our model. However, this comes with a limitation: the sampled hyperedge is constrained to have exactly k nodes. During training, this constrain helps the optimisation in terms of stability, allowing us to easily train our model without the need for regularisation or optimisation tricks. However, we are restricted to predict only k -regular hyperedges (i.e. hyperedges containing exactly k nodes). While in all our experiments we use the same constant k for all hyperedges, the framework allows us to use a sequence of cardinalities, ones for each hyperedge. However, additional domain knowledge is needed to pre-determined this sequence. Since having extra slots proved to be harmless for our model, one solution is to provide a diverse list of k such that it covers a broader range of possibilities. While interesting to explore, these experiments are left as future work.

In order to better align with the current literature, we mainly validate our model on the trajectory prediction task. However, in the current form, our model predicts a single hypergraph structure for

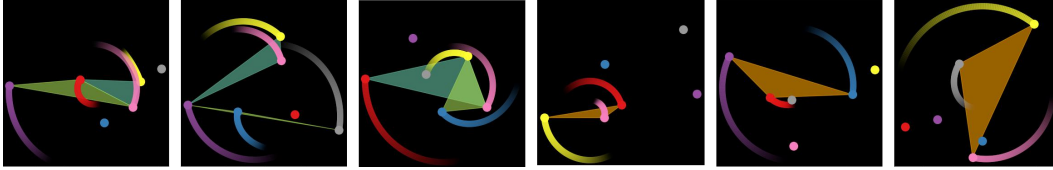


Figure 5: **Examples of 25-steps trajectories from the Particle Simulation datasets** for both the One-Triangle and the Two-Triangles variants. The highlighted triangles represent the 3-order interactions used to generate the trajectories.

the entire trajectory. This is well suited for the synthetic benchmark, where the dynamics for each example is determined by a single hypergraph structure, that does not change in time. On the other hand, in real-world setups, such as the NBA dataset, the higher-order interactions between the players might change along the game. Thus, having a distinct, dynamic hypergraph structure, that evolves in time, could be beneficial. However, solving trajectory prediction is not the main goal for our model. Instead, our purpose is to have a general model, that allows us to infer and process higher-order interaction. We believe that adapting SPHINX to more specific scenarios, such as creating a dynamic, evolving structure is an interesting area for future work.

B Visualisations

One of the advantages brought by our method is providing a discrete latent hypergraph structure, that can be easily visualise, offering a higher level of interpretability compared to attention-based methods. Figure 6 shows the trajectories and latent structure learned by our model on some examples from the Two-Triangles and NBA datasets. We are visualising the ground-truth trajectories, the trajectories and structure predicted by our full model, and the trajectories and learned structure corresponding to the model used in our ablation study: *SPHINX w/o sequential* and *SPHINX w Gumbel*.

When the slots are predicted in parallel, without access to the already predicted hyperedges (the model called *SPHINX w/o sequential*), the slots tends to collapse in a single hyperedge represented by all the slots. On the other hand, removing the constraints on the cardinality of the hyperedges, by applying Gumbel-Softmax (the model called *SPHINX w Gumbel*), the optimisation process leads to "greedy" slots, that covers all the nodes in the hypergraph.

In contrast, our *SPHINX* model learns sparse and intuitive hypergraph structures, alleviating the slot collapsing behaviour. On the synthetic dataset, the predicted hypergraph highly coincide with the real connectivity. By inspecting the higher-order structures learned by our model on the NBA dataset, we observe that most of the inferred hyperedges contains the node associated with the ball (denoted as a white node in Figure 6). we believe that this is a natural choice, since the position of the ball should have a critical influence on the decision taken by all basketball players.

C Experimental details

C.1 Datasets details

We create a synthetic benchmark, Particle Simulation, to validate the capabilities of our model in terms of downstream performance, while also enabling the evaluation of the predicted higher-order interactions. Previous works used various synthetic setups to achieve this goal. However, to our knowledge, none of them are publicly available.

Particle Simulation dataset contains a set of particles moving according to a higher-order law. Each example in our dataset consists of $N = 6$ particles moving in a 2D space. Among them, K random triangles where uniformly sampled to represent K 3-order interactions. All the particles that are part of a triangles are rotating around the triangle's center of mass with an angular velocity θ_i randomly sampled for each particle i . If one particle is part of multiple triangles, the rotation will happen around their average center of mass. The task is, given the first $t = 22$ time steps of the trajectory (only the position of the particles and the angle velocity associated with the particles, no triangles provided), to be able to predict the rest of the trajectory (25 steps). Note that, for each example in the

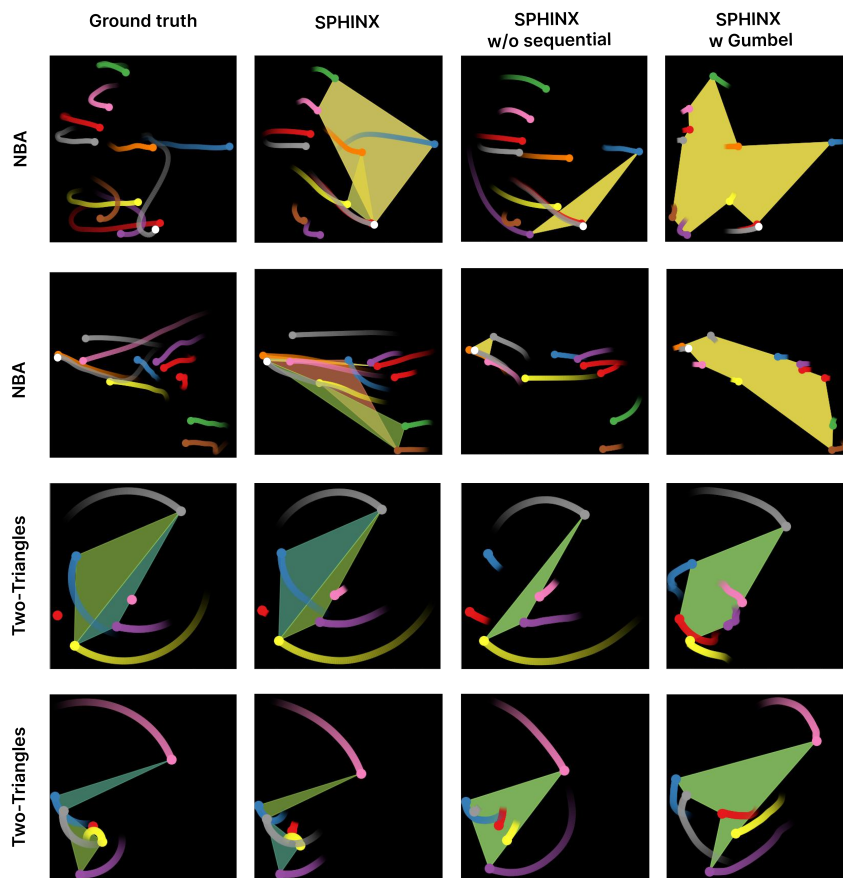


Figure 6: **Visualisation of the trajectories** predicted by our full model (SPHINX) and the two variations used in the ablation study (SPHINX w/o sequential and SPHINX w Gumbel) on the Two-Triangles and NBA dataset. In the ground-truth column the highlighted polygons represent the true connectivity, while for the models they represent the discovered hyperedges. Both using Gumbel-Softmax and dropping the sequential prediction clearly impact the predicted hypergraphs. On the other hand, our model manage to discover diverse structures, close to the ground truth ones in the synthetic scenario.

dataset, we have different triangles connecting the particles. Given the hypergraph structure, the task satisfy the Markovian property, but in order to predict the hypergraph structure you need access to at least 2 consecutive timesteps.

We create two variants of the dataset. A simpler one, containing a single higher-order interaction per trajectory (denoted as One-Triangle), and a more challenging one containing two higher-order interaction per trajectory (denoted as Two-Triangles). Each dataset contains 1000 training, 1000 validation and 1000 test trajectories.

Some examples of the datasets are depicted in Figure 5.

C.2 Implementation details

Model details. To encode the observed part of the trajectory into the hypergraph predictor, we are experimenting with two variants. Either we are using an MLP that receives the concatenation of the node’s coordinates from all timesteps, or a 1D temporal Convolutional Neural Network acting on the temporal dimension.

For the synthetic dataset, both the hypergraph predictor and the hypergraph processor are receiving as input the (x,y) coordinates of each node, while for the NBA dataset the spatial coordinates are enriched with information about the velocity (the real velocity for the observed trajectory and the estimated one during evaluation).

For the AllDeepSets model, used as Hypergraph Processor, we adapt the standard architecture, by incorporating information about the angular velocity θ_i at each layer, in the form of $\sin(\theta_i)$, $\cos(\theta_i)$ concatenated to each node at the end of each layer.

Unless otherwise specified, the results reported in the main paper are obtained using hyper-parameter tuning. We are performing bayesian hyperparameter tuning, setting the base learning rate at 0.001, multiplied with a factor of $d \in \{0.1, 1.0, 10.0\}$ when learning the parameters corresponding to the hypergraph predictor, a batch size of 128, self-loop added into the structure. The hidden state is picked from the set of values $\{32, 64, 128, 256\}$, the number of AllDeepSets layers from $\{1, 2\}$, the number of layers for the used MLPs from $\{2, 3, 4\}$, the number of hyperedges from $\{1, 2, 3, 5, 7\}$ (except for the synthetic setup where the number of hyperedges is set to 1 and 2 respectively), the dimension of hyperedges from $\{3, 4, 5, 6\}$ (except for the synthetic setup where the number of hyperedges is set to 3), nonlinearities used for the similarity score are either sigmoid, sparsemax or softmax, the algorithm for k -subset sampling is either AIMLE or SIMPLE, with their associated noise distribution sum of gamma or gumbel. For the NBA dataset, we are training for 300 epochs, while for the Particle Simulation we are training for 1000 epochs.

The code for loading the NBA dataset is based on the official code for [42]¹. The code for the various k -subset sampling algorithms is based on the code associated with AIMLE² [9], IMLE³ [46] and SIMPLE⁴ [8] methods.

Metric details. To validate to what extent our model is able to predict the correct hypergraph structure, we are computing the overlap between the predicted hypergraph and the ground-truth connectivity used to generate the trajectory. For a model predicting K hyperedges, let’s consider the set of predicted hyperedges as $P = \{p_1, p_2..p_K\}$ and the target hyperedges as $G = \{g_1, g_2..g_K\}$. For each element i , we are computing the percentage of the nodes that are in both the prediction p_i and the ground-truth hyperedge g_i . Since we are computing the element-wise overlap between two unordered sets, we fix the order of the ground-truth list G , and compute the metric against all the possible permutations of P . The overlap corresponding to the best permutation represents our reported metric. This metric is a scalar between 0 and 1, with 0 representing completely non-overlapping sets, and 1 denoting perfect matching.

Computational complexity. We analyse the computational complexity of the hypergraph-inference component for the SPHINX architecture (hypergraph predictor + sampling) when using the SIMPLE k -subset sampling algorithm. The overall complexity would be obtained by adding the complexity specific to the hypergraph neural network used to process the higher-order structure. If N is the number of nodes, K is the cardinality of the predicted hyperedges and M is the number of inferred hyperedges, the vectorized complexity for the sampling module is $O(\log N \times \log K)$ and the complexity of slot-attention with Q iterations and one slot is $O(Q \times N)$. Then, the overall complexity for predicting M hyperedges is $O(M \times Q \times N + M \times \log N \times \log K)$.

D Additional experiments

D.1 Full results on Particle Simulation

Due to page limits, in the main paper we only report the bar-plot for our synthetic experiments. Here we also include the numerical values (see Table 3 and Table 4), together with two additional models: one LSTM baseline, similar to the one proposed in [19], and a ground-truth-based oracle, to better understand the lower bound for our model.

In the following, we will describe all the baselines used in the Particle Simulations ablation study.

¹<https://github.com/MediaBrain-SJTU/GroupNet> - under MIT License

²<https://github.com/EdinburghNLP/torch-adaptive-imle> - under MIT License

³<https://github.com/uclnlp/torch-imle> under MIT License

⁴<https://github.com/UCLA-StarAI/SIMPLE> - custom License, open for research

Table 3: **Ablation study on the One-Triangle dataset.** Taking into account the higher-order interaction is crucial for predicting the trajectory. Both predicting the hyperedges sequentially and the constrained k -subset sampling are important for accurate hypergraph prediction.

Model	1 step	5 steps	25 steps
Golden standard	1.0e-8	1.0e-7	1.0e-6
Random structure	1.1e-4	1.1e-3	2.4e-2
No structure	1.1e-4	1.2e-3	2.4e-2
LSTM	2.0e-5	1.0e-1	1.7e-1
SPHINX w Gumbel	1.0e-4	1.0e-3	2.3e-2
SPHINX	3.6e-6	3.9e-5	1.1e-3

Table 4: **Ablation study on the Two-Triangles dataset,** reinforcing the conclusions from the One-Triangle dataset. Having a learnable hypergraph structure improves the trajectory prediction, while the constrained k -subset sampling is superior to Gumbel-Softmax. Moreover, the model further benefits from a sequential prediction of slots.

Model	1 step	5 steps	25 steps
Golden standard	4.0e-8	5.0e-7	9.0e-6
Random structure	1.1e-4	1.1e-3	2.0e-2
No structure	1.1e-4	1.2e-3	2.5e-2
LSTM	3.0e-5	9.5e-2	1.7e-1
SPHINX w/o sequen.	5.0e-5	5.0e-4	1.0e-2
SPHINX w Gumbel	1.0e-4	1.1e-3	2.5e-2
SPHINX	2.0e-5	2.0e-4	6.0e-3

Golden standard represents the lower bound in terms of MSE for our model. Instead of predicting the hypergraph structure, this model uses the ground-truth connectivity. The *oracle* hypergraph is then fed into the hypergraph neural network for predicting the next timestep. The purpose of this model is to understand what is the target performance we can aim for, while taking into account the possible limitation of the hypergraph processor (AllDeepSets in our case).

Random structure follows the same pipeline used to train the *Golden standard* baseline. However, instead of the ground-truth connectivity, this model uses a randomly sampled hypergraph. The goal is to understand how much of our performance comes from having a strong decoder, compared to the advantage of predicting a real, suitable hypergraph structure.

No structure entirely ignores the higher-order interaction, by setting the incidence matrix to zero. The purpose of this baseline is to understand to what extent our datasets require higher-order interactions.

LSTM. Inspired by the baselines in [19], we designed an LSTM-based [55] model which receives all the nodes concatenated, and predicts, at each timestep, the future coordinates for all the nodes. While capable of capturing relationships between nodes, this model doesn't have an inductive bias towards modelling higher-order interactions.

SPHINX w/o sequential uses the same processing as our full proposed model. However, instead of a sequential slot-attention, it uses the classical slot-attention clustering, which predicts all the slots simultaneously. Comparison with this baseline sheds light on the importance of predicting the hyperedges sequentially.

SPHINX w Gumbel is a modification of our full SPHINX model, by replacing the k -subset sampling with the Gumbel-Softmax, frequently used in both graph and hypergraph inference models. While allowing us to propagate gradients through the sampling step, the Gumbel-Softmax has no constraints on the number of nodes contained in each hyperedge, sampling independently for each node-hyperedge incidence relationship.

Results. Table 3 and Table 4 show the results of the ablation study on both the One-Triangle and Two-Triangles datasets. Compared to the model using either perturb structure (*Random structure*) or the one completely ignoring the higher-order connectivity (*No structure*), our model shows clearly advantage on both datasets, showing that learning to infer the hypergraphs is a critical step in the higher-order processing pipeline. Moreover, all the experiments show a clear advantage for the k -subset sampling compared to the classical Gumbel-Softmax, with the sequential prediction further increasing the performance. The LSTM baseline performs well on the next step prediction task, but the performance deteriorates severely on the medium (5 steps) and long-range prediction (25 steps). It is interesting to notice that, even if the model discovers the hypergraph structure almost perfectly (see Figure 4 in the main paper), there is still a gap in performance between our learnable SPHINX and the Golden standard model.

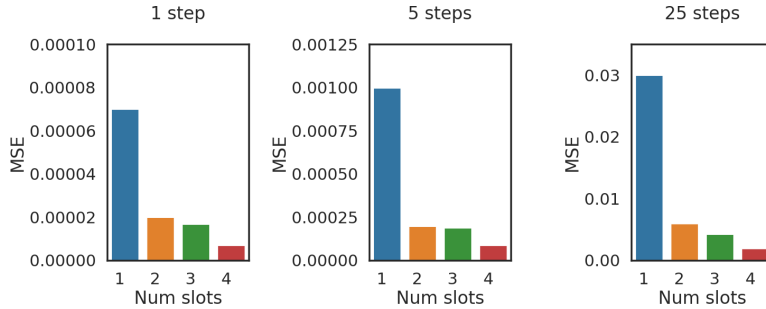


Figure 7: **Experiments on Two-Triangles dataset investigating the importance of choosing the correct number of predicted hyperedges.** Having less hyperedges than the real number (two) negatively impact the performance. However, when increasing the number of hyperedges above the true value, the performance does not deteriorate, indicating that the model is robust at discovering the hypergraph structure, as long as enough slots are provided.

D.2 Varying number of hyperedges

Although the number of parameters does not scale with the number of inferred hyperedges, by construction we are restricted to predict maximum M hyperedges, where M is set as hyperparameter. This is mainly due to the use of binary feature vector b encoding the history predicted so far, which has a fixed dimension $\{0, 1\}^{N \times (M-1)}$.

To establish to what extent the value we choose as the number of hyperedges impacts the performance, we conduct an ablation study by varying the number of slots predicted by our method. The results in Figure 7 show that picking a number of slots larger than the real one doesn't harm the performance. Visual analysis of the learned hypergraph reveals that, when offering more slots than needed, the model tends to produce redundancy, associating the extra slots to hyperedges that were already discovered.